

ChemComm

Accepted Manuscript



This is an *Accepted Manuscript*, which has been through the Royal Society of Chemistry peer review process and has been accepted for publication.

Accepted Manuscripts are published online shortly after acceptance, before technical editing, formatting and proof reading. Using this free service, authors can make their results available to the community, in citable form, before we publish the edited article. We will replace this *Accepted Manuscript* with the edited and formatted *Advance Article* as soon as it is available.

You can find more information about *Accepted Manuscripts* in the [Information for Authors](#).

Please note that technical editing may introduce minor changes to the text and/or graphics, which may alter content. The journal's standard [Terms & Conditions](#) and the [Ethical guidelines](#) still apply. In no event shall the Royal Society of Chemistry be held responsible for any errors or omissions in this *Accepted Manuscript* or any consequences arising from the use of any information it contains.

Cite this: DOI: 10.1039/c0xx00000x

www.rsc.org/xxxxxx

Communication

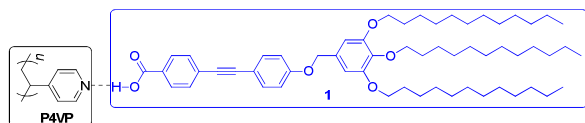
Complex of Poly(4-vinylpyridine) and Tolane Based Hemi-phasmid Benzoic Acid: Towards Luminescent Supramolecular Side-Chain Liquid Crystalline Polymer

Shao-Jie Wang,^a Rui-Ying Zhao,^a Shuang Yang,^a Zhen-Qiang Yu,^{*b} and Er-Qiang Chen^{*a}

Received (in XXX, XXX) Xth XXXXXXXXX 20XX, Accepted Xth XXXXXXXXX 20XX
DOI: 10.1039/b000000x

Supramolecular side-chain liquid crystalline (LC) polymer P4VP(1)_x was prepared using poly(4-vinylpyridine) and a tolane based hemi-phasmid benzoic acid. P4VP(1)_x exhibits good processability, forming smectic and hexagonal columnar LC phases at different compositions. Its photoluminescent property depends on the LC structures.

To create functional materials in the “rapid optimization” manner, the strategy of supramolecular chemistry has been widely explored in the past years.¹ Considering a linear polymer which can provide the non-covalent interaction sites along the chain, introducing small molecules bearing complementary recognition units to the polymer can result in a supramolecular side-chain polymer (SCP).² Owing to the dynamic nature and diversities of molecular design, the functionality of supramolecular SCP can be easily tuned by selecting appropriate polymer chains and small molecules. Using intermolecular hydrogen bonding interaction, Kato and Fréchet first synthesized non-covalent side-chain liquid crystalline (LC) polymers.³ After this pioneer work, great progress has been achieved in the field of supramolecular SCP. Other than hydrogen bonding,⁴ electrostatic interaction⁵ and metal-ligand coordination interaction⁶ have also been employed. It is realized that addition of the non-mesogenic ligand can induce a lamellar phase of the polymer-ligand complex, wherein the nano-segregation between the polar and non-polar components plays a key role.⁷ Once the supramolecular SCP is incorporated into block copolymers, complex hierarchical structures can be obtained.⁸ With the superior processability and mechanical property offered by the polymer chains, the non-covalent SCP in solid state shall possess great potentials in applications as functional materials.



Scheme 1. Complex of P4VP(1)_x based on hydrogen bonding interaction.

Here we report a supramolecular side-chain LC polymer based on the intermolecular hydrogen bonding between poly(4-vinylpyridine) (P4VP) and a benzoic acid derivative **1** (Scheme 1). It is worthy to note that the dimer of **1** is in fact a phasmid LC with a rodlike mesogen ending with two half-disk moieties.⁹ In

this context, molecule **1** can be viewed as a hemi-phasmid. Phasmid mesogens exhibit fascinating self-assembly behaviour, forming frequently columnar LC phases. Using solution blending, we prepared the complex of P4VP(1)_x (*x* is a molar ratio of **1** to the repeating unit of 4VP). **1** contains a typical fluorescent mesogenic unit of tolane. Taking the advantage of complexation of P4VP and **1**, we intend to obtain a fluorescent system with improved processability in solid state. Experiments indicate that hydrogen bonding interaction between pyridine and the benzoic acid head of **1** can completely suppress the self-assembly of **1** at *x* ≤ 0.7. Increasing the content of **1** can lead to a change from smectic (Sm) to hexagonal columnar (Col_h) phase of P4VP(1)_x. With the help of P4VP, free-standing films of P4VP(1)_x were obtained. Both the Sm and Col_h can be well oriented by mechanical shearing. Also, we find that fluorescent property of the complex has a clear dependence on the phase structure.

Compound **1** itself rendered an enantiotropic phase behaviour, with three transitions and the isotropization temperature of 97 °C detected by differential scanning calorimetry (DSC) (Fig. S1, ESI). X-ray diffraction (XRD) revealed that **1** was crystalline at room temperature (Fig. S2), of which the first order diffraction located at *q* = 1.31 nm⁻¹ (*q* = 4πsinθ/λ, where 2θ is the scattering angle and λ the X-ray wavelength). For P4VP(1)_x with *x* > 0.7, the phase behaviour of pure **1** could be detected experimentally. However, when *x* ≤ 0.7, DSC results showed only one glass transition of the complexes (Fig. S3) before **1** was damaged at above 160 °C. The glass transition temperature (*T*_g) decreased from 142 °C for *x* = 0 to 82 °C for *x* = 0.7, suggesting that **1** could well complex with P4VP and also provide the plasticization effect. Compared to that between the benzoic acid groups, the hydrogen bonding between pyridine and benzoic acid is stronger. While the pyridine content is exceeded (i.e., *x* ≤ 0.7) in the mixture, the balance shifts towards the P4VP(1)_x complex formation. The hydrogen bonding interaction of pyridine/benzoic acid can be confirmed by FT-IR (Fig. S4).

Fig. 1a presents the XRD profiles of P4VP(1)_x with various contents of **1** at room temperature (also see Fig. S5). With a very small *x* of 0.05, P4VP(1)_x presents a broad scattering peak at round *q* of 0.5 nm⁻¹, suggesting no ordered phase formed. When *x* exceeds 0.7, careful examination can reveal the diffractions of the pure **1** in addition to that of P4VP(1)_x. For 0.1 ≤ *x* ≤ 0.7, P4VP(1)_x could exhibit LC texture under polarized optical

microscopy (Fig. S6), and give multiple diffractions in the low-angle region. Two diffractions with q -ratio of 1:2 are observed when $x < 0.3$, indicative of Sm (or lamellar) phase. Increasing x can result in the low-angle diffractions of a Col_h phase, of which the q -ratio follows 1: $\sqrt{3}$:2. Consequently, a change from Sm to Col_h is induced by increasing x , similar to that reported previously.¹⁰ We consider that while the heads of **1** molecules are prone to attaching to the pyridine along the P4VP chains, addition of **1** can cause the density fluctuation first and then lead to the ordered structure. Owing to the overall incompatibility of the two components, the Sm structure shall involve two sublayers composed primarily of **1** and P4VP, respectively. The interface of sublayers should be diffusive at $x = 0.1$, evidenced by the relatively broad peaks. Adding more **1** makes the Sm diffraction sharper, implying better microphase separation. When even more **1** molecules participated in the complexation, more binding sites of pyridine are required to expose on the interface. This can cause the interface curved, and thus the formation of Col_h phase.

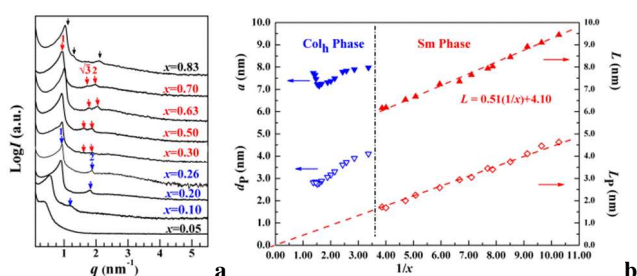


Fig. 1 (a) 1D XRD profile of P4VP(**1**)_x with various x ranging from 0.05 to 0.83. The blue and red arrow indicate the Sm and Col_h diffractions. The black arrow points to the diffraction coming from the crystal of pure **1**. (b) Dimensions (solid symbols) of Sm and Col_h phase as functions of $1/x$. The sizes of P4VP domains (open symbols) in the LC phases are also plotted. L_p represents the thickness of P4VP sublayer in the Sm phase. d_p denotes the diameter of P4VP cylindrical domain in the Col_h phase.

The d -spacings corresponding to the first order diffraction in the low-angle region of P4VP(**1**)_x are shown in Fig. S7. Fig. 1b plots the layer spacing of Sm (L) and a parameter of Col_h as functions of the reciprocal of x . It is found that $L \propto 1/x$, same as that in other lamellar phases of polymer-surfactant systems.⁷ This linear relationship suggests that the Sm phase formation is based on microphase separation of **1** and P4VP. The data fitting gives the intercept of 4.1 nm, rather close to the extended length of 3.8 nm of **1**, implying that the Sm structure is monolayer smectic A with the rodlike mesogen of tolane largely parallel to the Sm layer normal (Fig. S8). Assuming that the P4VP and **1** sublayers possess approximately the densities of 1.2 and 1 g cm⁻³,^{7b} respectively, we can estimate the thicknesses of the two sublayers based on a simple volumetric argument (details see ESI). As shown in Fig. 1b, the P4VP sublayer thickness (L_p) decreases from 4.6 to 1.8 nm, indicating that the P4VP chains therein are subjected to an enhanced confinement when x is increased. Further compressing the P4VP chains to be more oblate in the Sm sublayer will be thermodynamically unfavourable.

For the Col_h phase, as the volume fraction of **1** is much larger than that of P4VP, P4VP chains shall form cylindrical domains embedded in the matrix of **1** with a hexagonal symmetry. The diameter of P4VP cylinder decreases with x , reaching ~ 2.8 nm at x of ~ 0.6 (Fig. 1b). Note that the a of Col_h is obviously smaller

than twice the extended length of **1**. The alkyl tails of **1** shall assume coiled and may interdigitated pack to full fill the space. Moreover, the **1** molecules tethered on the P4VP cylinder surface via hydrogen bond also tilt with respect to the column axis (Fig. S9). At $x > 0.65$, the a parameter increases, implying that the Col_h phase can be swelled by **1** to some extent. However, when $x > 0.7$, newly added **1** molecules will be expelled from the LC domains.

The schematics of the Sm and Col_h are shown in Fig. 2a and 2b, respectively. Thermal XRD results indicated that both of the LC phases could maintain up to 150 °C (Fig. S10). Free-standing films of the LC P4VP(**1**)_x can be obtained after solution casting. At above T_g , the samples can be well oriented by mechanical shearing. Fig. 2c and 2d present the low-angle two-dimensional (2D) XRD patterns of P4VP(**1**)_{0.15} and P4VP(**1**)_{0.45} recorded at room temperature with the X-ray incidence parallel to the shear direction. In Fig. 2c, the layer diffraction is on the meridian (the shear gradient), indicating that P4VP(**1**)_{0.15} has its Sm layer normal perpendicular to the shear direction. For P4VP(**1**)_{0.45} with Col_h phase, diffractions with the 6-fold symmetry up to the third order can be clear detected. This demonstrates that not only the cylinders can be well aligned along the external force direction, but also the rotational disorder around the column axis is largely suppressed. We attempted to orient the pure **1** by mechanical shearing, but the result was always unsatisfied. As P4VP(**1**)_x can be readily aligned, obviously, the P4VP chains play a key role here, which offer the complex with good processability.

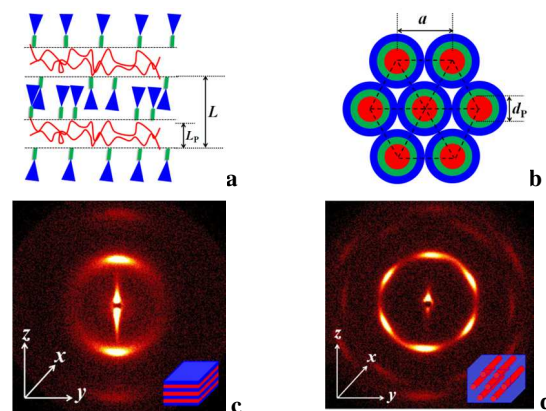


Fig. 2 (a) and (b), Schematics of monolayer Sm and Col_h phase. (c) and (d), Low-angle 2D XRD patterns of P4VP(**1**)_{0.15} and P4VP(**1**)_{0.45}. The axes of x and z indicate the shear direction and shear gradient. The 2D patterns were recorded with X-ray beam parallel to the shear direction.

Reports show that many tolane derivatives are non-emissive when molecularly dissolved in good solvent, but emit intensely when aggregated in poor solvent or in solid state, which is caused by the restricted intramolecular rotations in aggregate state.¹¹ Containing a bulky half-disk moiety, **1** has its intramolecular rotations restricted to a certain extent in solution state and thus is highly emissive. The photoluminescent quantum yield (Φ) of molecule **1** measured was up to 0.36 in chloroform. However, in solid state, the Φ value of the pure **1** was only of ~ 0.04 , implying the fluorescent quenching occurred due to the H-aggregation in the crystalline state of **1**.¹² Here, of particular interest is to compare the photophysical behaviour of P4VP(**1**)_x films with that of the pure **1** film. We anticipate that the LC structure will improve the emission of **1** in solid state.

As shown in Fig. 3a, the maximum absorption wavelength of P4VP(**1**)_{0.40} film shifts to 313 nm relative to that of 323 nm for the **1** film. This hypsochromic shift suggests that complexation of **1** with P4VP can lead to the de-association of H-aggregation of **1**. On the other hand, the emission of the complex peaks at a longer wavelength of 404 nm. Importantly, **1** molecules in P4VP(**1**)_x exhibit higher Φ once its crystalline packing was destroyed (Fig. 3b). In the disordered phase or at the beginning of Sm phase of P4VP(**1**)_x ($x \leq 0.1$), **1** molecules likely dissolve in the glassy P4VP and can give the Φ value of ~ 0.13 , much higher than that of the **1** film. Fig. 3b shows that the Φ of P4VP(**1**)_x declines with increasing x , which should be mainly due to the decreased distance between neighbouring tolane groups. Interestingly, the Φ dependence on x can be well correlated with the phase structures. Namely, with x of ~ 0.3 as the boundary, two stages of Φ drop are observed, corresponding to the Sm and Col_h phase, respectively. It is worth mentioning that in the Sm phase with a monolayer structure many of the **1** molecules are anti-parallel to each other (Fig. 2a). This interdigitated packing largely prevents the H-aggregation. For the Col_h phase, the **1** molecules surrounding a P4VP column are aligned nearly along the radial direction. Considering a stratum of cylinder, when more **1** molecules are inserted therein, the two neighbouring tolanes will have their angle and lateral distance reduced.¹³ Consequently, the Φ decreases, and eventually, the Col_h phase at $x = 0.7$ renders the Φ rather close to the pure **1** film.

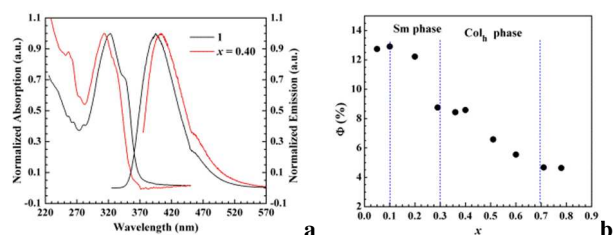


Fig. 3 (a) Thin film UV-Vis absorption and fluorescence spectra of **1** and P4VP(**1**)_{0.40}. (b) Quantum yield of P4VP(**1**)_x with various x .

Conclusions

In summary, to obtain a luminescent supramolecular side-chain LC polymer with good processability, we made the complex of P4VP(**1**)_x based on intermolecular hydrogen bond. Crystallization of the hemi-phasmid **1** bearing tolane moiety can be completely suppressed when the molar ratio x of **1** to 4VP is lower than 0.7. Increasing x causes the LC phase of P4VP(**1**)_x changing from Sm to Col_h. The LC complex can be well oriented by shearing. The solid films of P4VP(**1**)_x exhibit luminescent emission stronger than the pure **1**, of which the quantum yield depends on the LC phase structures. This demonstrates that manipulating the phase structure is an effective and facile way to tune the property of supramolecular SCPs as functional materials.

This work was supported by the National Natural Science Foundation of China (20990232, 21104001, and 21074073).

Notes and references

^a Beijing National Laboratory for Molecular Sciences, Key Laboratory of Polymer Chemistry and Physics of Ministry of Education, College of Chemistry and Molecular Engineering, Peking University, Beijing, China. E-mail: eqchen@pku.edu.cn.

^b School of Chemistry and Chemical Engineering, Shenzhen Key Laboratory of Functional Polymers, Shenzhen University, Shenzhen 518060, China; E-mail: zqyu@szu.edu.cn

[†] Electronic Supplementary Information (ESI) available: [Materials and instruments, materials synthesis, DSC and XRD of **1**, DSC, XRD, and POM of P4VP(**1**)_x with various x]. See DOI: 10.1039/b000000x/

- (a) J. M. Lehn, *Angew. Chem. Int. Edit.*, 1990, **29**, 1304. (b) J. Pollino and M. Weck, *Chem. Soc. Rev.*, 2005, **34**, 193. (c) M. Hammond and R. Mezzenga, *Soft Matter*, 2008, **4**, 952.
- (a) T. Kawakami, T. Kato, *Macromolecules*, 1998, **31**, 4475. (b) M. Gopinadhan, E. S. Beach, P. T. Anastas and C. O. Osuji, *Macromolecules*, 2010, **43**, 6646. (c) Z. Cheng, B. Ren, D. Zhao, X. Liu and Z. Tong, *Macromolecules*, 2009, **42**, 2762.
- (a) T. Kato and J. M. J. Frechet, *Macromolecules*, 1989, **22**, 3818. (b) T. Kato, N. Mizoshita and K. Kishimoto, *Angew. Chem. Int. Edit.*, 2006, **45**, 38.
- (a) L. Bouteiller, *Adv. Polym. Sci.*, 2007, **207**, 79. (b) G. Ten Brinke, J. Ruokolainen and O. Ikkala, *Adv. Polym. Sci.*, 2007, **207**, 113. (c) H. Sun, C. Lee, C. Lai, H. Chen, S. Tung and W. Chen, *Soft Matter*, 2011, **7**, 4198. (d) J. de Wit, G. A. van Ekenstein, E. Polushkin, K. Kvashnina, W. Bras, O. Ikkala and G. Ten Brinke, *Macromolecules*, 2008, **41**, 4200. (e) C.-Y. Chao, X. Li, C. K. Ober, C. Osuji and E. L. Thomas, *Adv. Funct. Mater.*, 2004, **14**, 364.
- (a) C. K. Ober and G. Wegner, *Adv. Mater.*, 1997, **9**, 17. (b) C. F. J. Faul and M. Antonietti, *Adv. Mater.*, 2003, **15**, 673. (c) Y. Cheng, W. Chen, C. Zheng, W. Qu, H. Wu, Z. Shen, D. Liang, X. Fan, M. Zhu and Q. Zhou, *Macromolecules*, 2011, **44**, 3973. (d) U. H. Yildiz, K. Koynov and F. Gröhn, *Macromol. Chem. Phys.*, 2009, **210**, 1678. (e) Q. A. Zhang and C. G. Bazuin, *Macromol. Chem. Phys.*, 2010, **211**, 1071. (f) M. Antonietti, J. Conrad, and A. F. Thunemann, *Macromolecules*, 1994, **27**, 6007.
- (a) U. S. Schubert and C. Eschbaumer, *Angew. Chem. Int. Ed.*, 2002, **41**, 2892. (b) I. Welterlich and B. Tiek, *Macromolecules*, 2011, **44**, 4194. (c) S. Valkama, T. Ruotsalainen, H. Kosonen, J. Ruokolainen, M. Torkkeli, R. Serimaa, G. Brinke, and O. Ikkala, *Macromolecules* 2003, **36**, 3986.
- (a) G. Ten Brinke, J. Ruokolainen and O. Ikkala, *Europhys. Lett.*, 1996, **35**, 91. (b) J. Ruokolainen, M. Torkkeli, R. Serimaa, S. Vahvaselkä, M. Saariaho, G. Ten Brinke and O. Ikkala, *Macromolecules*, 1996, **29**, 6621.
- (a) C. Osuji, C. Y. Chao, I. Bitá, C. K. Ober and E. L. Thomas, *Adv. Funct. Mater.*, 2002, **12**, 753. (b) J. Ruokolainen, R. Mäkinen, M. Torkkeli, T. Makela, R. Serimaa, G. Ten Brinke and O. Ikkala, *Science*, 1998, **280**, 557. (c) H. Kosonen, J. Ruokolainen, M. Knaapila, M. Torkkeli, K. Jokela, R. Serimaa, G. Ten Brinke, W. Bras, A. P. Monkman and O. Ikkala, *Macromolecules*, 2000, **33**, 8671. (d) Y. Zhao, K. Thorkelsson, A. J. Mastroianni, T. Schilling, J. M. Luther, B. J. Rancatore, K. Matsunaga, H. Jinnai, Y. Wu, D. Poulsen, J. M. J. Frechet, A. P. Alivisatos and T. Xu, *Nature Mater.* 2009, **8**, 979. (e) B. J. Rancatore, C. E. Mauldin, S. H. Tung, C. Wang, A. Hexemer, J. Strzalka, J. Frechet and T. Xu, *Acs Nano*, 2010, **4**, 2721.
- (a) H.-T. Nguyen, C. Destrade and J. Malthete, *Adv. Mater.* 1997, **9**, 375. (b) B. P. Hoag and D. L. Gin, *Adv. Mater.* 1998, **10**, 1546. (c) M. Gharbia, A. Gharbi, H. T. Nguyen and J. Malthete, *Curr. Opin. Colloid Interface Sci.* 2002, **7**, 312-325.
- (a) X. Zhu, U. Beginn, M. Moller, R. I. Gearba, D. V. Anokhin and D. A. Ivanov, *J. Am. Chem. Soc.*, 2006, **128**, 16928. (b) S. J. Wang, Y. S. Xu, S. Yang and E. Q. Chen, *Macromolecules*, 2012, **45**, 8760.
- (a) J. D. Luo, Z. L. Xie, J. W. Y. Lam, L. Chen, H. Y. Chen, C. F. Qiu, X. W. Zhan, Y. Q. Liu, D. B. Zhu and B. Z. Tang, *Chem. Commun.* 2001, 1740; (b) Y. N. Hong, J. W. Y. Lam and B. Z. Tang, *Chem. Commun.* 2009, 4332; (c) Y. F. Chen, J. S. Lin, W. Z. Yuan, Z. Q. Yu, J. W. Y. Lam and B. Z. Tang, *Sci China Chem*, 2013, **56**, 1191.
- (a) H. Z. Liu, J. Mack, Q. L. Guo, H. Lu, N. Kobayashi and Z. Shen, *Chem. Commun.* 2011, **47**, 12092. (b) X. Zhang, D. Görl, V. Stepanenko and F. Würthner, *Angew. Chem. Int. Ed.* 2014, **53**, 1270.
- J. Cornil, D. Beljonne, J.-P. Calbert and J.-L. Bredas, *Adv. Mater.* 2001, **13**, 1053.